A variable-angle spectroscopic ellipsometry study of the effect of First Contact polymer on XeF_2-passivated MgF_2 thin-film aluminum mirrors

Lauren W. Miner

A senior thesis submitted to the faculty of
Brigham Young University
in partial fulfillment of the requirements for the degree of

Bachelor of Science

David D. Allred, Advisor

Department of Physics and Astronomy

Brigham Young University

Copyright © 2026 Lauren W. Miner

All Rights Reserved

ABSTRACT

A variable-angle spectroscopic ellipsometry study of the effect of First Contact polymer on XeF_2-passivated MgF_2 thin-film aluminum mirrors

Lauren W. Miner
Department of Physics and Astronomy, BYU
Bachelor of Science

Magnesium fluoride on xenon difluoride-passivated aluminum (Al+$XeMgF_2$) is a key candidate for space telescopes and satellites that require both far-UV (FUV) measurements and high reflectance at longer wavelengths. Contamination can significantly reduce FUV reflectance, so Al+$XeMgF_2$ mirrors must be kept as clean as possible. Protecting the surfaces during storage is also desirable. We investigated the suitability of four different formulations of Photonic Cleaning Technologies' First Contact Polymer for cleaning and protecting Al+$XeMgF_2$ coatings through repeated cleaning tests. All of the formulations were able to clean samples at least once. Using variable-angle, spectroscopic ellipsometry (VASE), we found that two of the four formulations (S2 and S3) were able to clean the Al+$XeMgF_2$ surfaces multiple times (over 20 cleaning cycles) and protect the surface for over 13 months without detectable alumina growth on the aluminum in a low-humidity environment. The samples were cleaved from a silicon wafer coated with 300 nm of chemical vapor deposited (CVD) silicon nitride (Si_3N_4). The thickness of the apparent MgF_2 layer also remained unchanged. "Apparent MgF_2" includes the deposited MgF_2, the 2–3 nm AlF_3 layer produced by the XeF_2 passivation step, and contributions from surface roughening. No detectable alumina growth was observed for the control samples. Overall, the results show that Al+$XeMgF_2$ coatings can be successfully cleaned, protected, and stored under certain First Contact formulations for at least 13 months in a dry environment.

Keywords: First Contact polymer, aluminum, magnesium fluoride coating, space telescope mirror, ellipsometry

ACKNOWLEDGMENTS

I would like to acknowledge NASA SBIR (Contract #80NSSC24PB405) for partially funding this research. I thank Dr. Manuel Quijada, Javier del Hoyo, Edward Wollack, and Mateo Batkis at NASA Goddard, as well as Dr. Luis Rodiguez de Marcos at the Catholic University of America, for providing the Al+XeMgF2 samples used in this study.

I gratefully acknowledge the J.A. Woollam Co., Inc., which provided several one-year licenses of their CompleteEase software. This allowed me to analyze the many Ψ and Δ files this study generated. This work, including RA funding, was provided by the Department of Physics and Astronomy and the College of Computation, Mathematics, and Physical Sciences of Brigham Young University.

I would like to thank Dr. James Hamilton from Photonic Cleaning Technologies for providing the First Contact polymer as well as consulting on the results I received from the experiment.

I'd like to acknowledge Joshua Vawdrey and Dr. Allred, who were big contributors to obtaining data as well as the analysis of data. They spent a considerable amount of time advising on this topic and suggesting edits to the overall document. I am grateful for their guidance.

Contents

List of Figures

Chapter 1

Introduction

Magnesium fluoride on xenon difluoride-passivated aluminum (Al+$XeMgF_2$) is a thin-film coating that enables aluminum, a material notable for its broad reflective range spanning the infrared to the ultraviolet, to maintain high reflectance, including in the far ultraviolet (FUV) range [1]. Maintaining high FUV reflectance is challenging because contamination or surface degradation can significantly reduce mirror performance, which is important for space-based optical applications. To address this challenge, First Contact polymer, developed by Photonic Cleaning Technology, offers a method for cleaning sensitive optical surfaces without damaging the coating.

1.1 FUV Reflectance

In this section, we discuss how to best achieve FUV reflectance. This includes using aluminum with a protective fluoride capping layer and keeping your mirror surface free from particulate contaminants and molecular residues through proper cleaning.

The wavelength range from the Lyman limit (91.2 nm) to the H Lyman-α (121.6 nm) is crucial to far-ultraviolet (FUV) astrophysical research. This region is especially valuable because it contains a rich concentration of spectral lines, providing astronomers with diagnostics of gas over a wide range of temperatures, ionization states, and densities. This has been increasingly important for characterizing exoplanet host stars, which is essential for correctly interpreting exoplanet atmospheric biosignatures [2].

To capture light between the Lyman limit and H Lyman-α, the state-of-the-art mirror coating options rely on the high FUV reflectance of aluminum (Al) [3]. However, Al oxidation after coating is nearly instantaneous upon exposure to air. This oxidation forms an Al_2O_3 layer that absorbs FUV photons and significantly decreases reflectivity in this wavelength range. To mitigate oxidation of the aluminum, a metal fluoride capping thin-film layer with a high bandgap is deposited on top of the aluminum layer. These fluorides act as a barrier to oxygen and moisture while being transparent in the FUV.

For this experiment, we used MgF_2 as our capping layer. MgF_2 is widely used for ultraviolet optics because of its high bandgap and low absorption. It also forms a stable protective film over aluminum. As a coating, MgF_2 for mirrors has shown promise in protecting mirrors against contamination and degradation. For example, the Hubble Space Telescope employed a MgF_2 coating, which was predicted to have less than 10% loss of reflectance at H Lyman-α due to contamination during ground-based operations [4].

1.2 Contamination Control

Another important factor in maximizing FUV reflectance is contamination control. Even small amounts of particulate matter or molecular films can introduce scattering or absorption losses, which are both detrimental at short wavelengths. When cleaning a mirror surface that will be used in a space telescope, it is important to remove the particulate contaminants and molecular residues. The ability to clean mirrors reliably and consistently to the atomic level is essential for meeting reflectance specifications. In addition, mirror coatings may remain in storage for extended periods before use, so protection from degradation is also required [5].

To address these challenges, Photonic Cleaning Technologies' Apply-Dry-Peel First Contact^{TM}. Polymers (FCP) can be used as a precision cleaning method. FCP is formulated to remove surface contaminants through an apply-dry-peel mechanism that is designed to lift particulates and molecular films without damaging the optical coating. Prior studies have shown that FCP can clean conventional mirrors of particles and molecular contaminants down to the angstrom level [6].

Similar experiments to the one presented in this paper were previously performed at BYU using Al+XeLiF coatings, and the results were published in a paper [7]. In those studies, Vawdrey found that while all the FCP formulations used were effective for single-use cleaning, none of the current formulations were suited for multiple cleanings or long-term storage. The results indicate that to achieve multiple cleanings and maintain stable storage, a new, custom-made formulation would need to be created for the Al+XeLiF-coated mirrors.

In our experiment, which builds directly on this prior work, we tested four formulations (S1-S4) of the FCP on Al+XeMgF_2-coated mirror samples. Our goals were to examine whether these formulations could perform repeated peel-off cleanings without degrading the mirrors and to evaluate their behavior under low-humidity storage conditions. To maintain continuity with the Al+XeLiF study, we used the same four formulations found in that paper [7]. This comparison between Al+XeLiF and Al+XeMgF_2 helps determine whether the performance limitations observed in that previous experiment persist when a different fluoride capping layer is used. Ellipsometry was chosen as the method for measuring changes in the thin-film stack because it is non-invasive, can be performed quickly, and offers sub-angstrom resolution.

Our results showed that we do find different results than the conclusions made in the Al+XeLiF study. Two of the four formulations (S2 and S3) were suited for long-term storage and repeated cleaning for Al+XeMgF_2 mirrors. These two formulations kept the MgF_2 layer thickness close to constant as well as minimized the alumina growth.

This paper first outlines how FCP was applied to each sample. Then it describes how ellipsometry and modeling were used to analyze changes in an Al+XeMgF_2 thin-film stack, providing insight into how these mirrors may perform in future space applications. Finally, the results of how the thin-film stack changed over a period of approximately 400 days will be presented and discussed.

Chapter 2

Methods

This chapter outlines the samples used in our experiment, as well as how we analyzed the changes being made to our thin-film stack. This includes the effects from multiple peel-offs and the storage effects of First Contact. There will be discussion on sample preparation, ellipsometry data, atomic force microscopy (AFM) data, and CompleteEASE modeling. All experiments were done at BYU facilities.

2.1 Sample Preparation

To get our desired thin-film stack for the experiment, we started with a 200-mm diameter silicon wafer (100 orientation), which was cleaved at BYU to produce a roughly square wafer piece measuring approximately 150 mm x 150 mm. This wafer piece had an approximately 300 nm chemically vapor deposited (CVD) Si_3N_4 coating to aid in ellipsometry characterization. The Al+XeMgF_2 layers were deposited at NASA GSFC [3], after which the wafer piece was returned to BYU.

Samples measuring about 1" x 1" were cleaved for the peel-off/storage experiments. Fig. 2.1 shows a cross section of the anticipated layers of the sample as well as the layer thicknesses used in

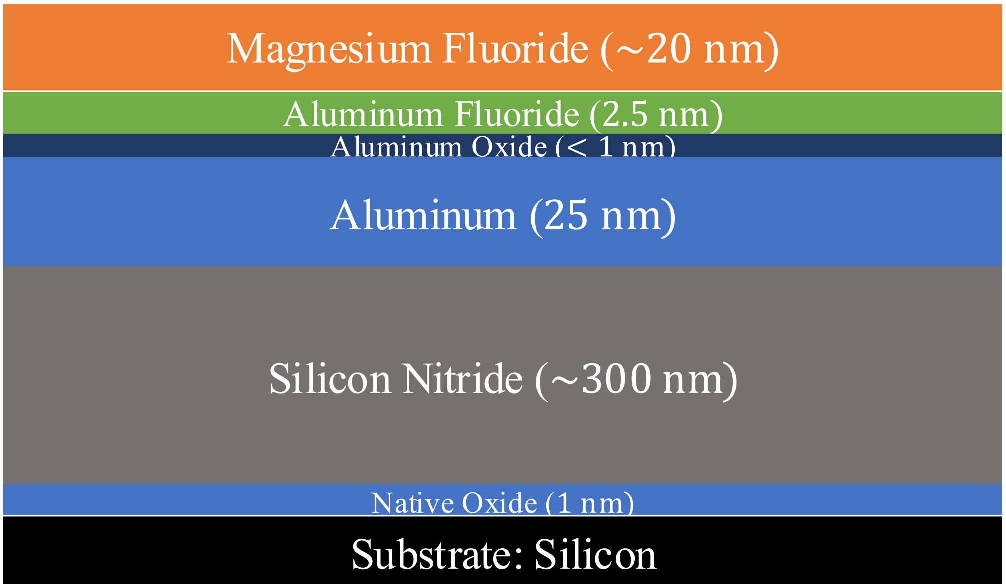

Figure 2.1 Model of the thin-film stack of the Al+XeMgF_2 used in this study. Al is deposited by vacuum evaporation, and AlF3 is formed from a XeF_2 passivation process, which immediately follows the Al deposition. Without breaking vacuum, MgF_2 is deposited by evaporation as a capping layer.

ellipsometry calculations. Note that the aluminum was made about 70% thinner than on standard flight mirrors, which allowed the ellipsometers' light to penetrate through the whole thin-film stack sufficiently to produce thin-film interference effects. This allowed us to analyze all changes in the thin-film layers. The aluminum oxide layer thickness was assumed to be about zero upon fabrication and upon our receiving the sample.

2.2 Cleaning and storage of samples

We define a 'peel-off cycle' as a process consisting of the following steps: (1) removing the FCP layer, (2) performing three to six ellipsometry measurements at different locations on the sample, (3) applying a specific FCP formulation on the surface of the Al+XeMgF_2, and (4) storing the sample in a desiccator maintained at <18% relative humidity (RH) until the designated time for step 1 to be repeated or for the FCP to be removed. This cycle allowed us to study the cleaning effects of First Contact as well as the storage effect between each 'peel-off cycle'. Four different formulations of FCP were used to clean four samples (S1-S4). The Red formulation was applied to S1, the Water-Resistant formulation to S2, the Gold formulation to S3, and the EUV formulation to S4. Samples S5 and S6 were not treated with FCP and served as controls.

2.3 Ellipsometry

To perform ellipsometry, we used a J.A. Woollam RC-2 variable-angle spectroscopic ellipsometer (VASE). VASE measures how light reflects from a surface in order to determine film thickness. The ellipsometer was used to understand how our thin-film stack (Figure 2.1) was changing [8].

The sample was measured three times along a line running through its center. In the majority of the measurements, the sample was then rotated 90° clockwise, and three additional measurements were performed. This gave a total of six spectroscopic ellipsometer (SE) measurements for that cycle. Taking six measurements allowed us to analyze any directional variations across the film. We started measuring six measurements for each peel-off cycle after day 5.

Each SE measurement consisted of multiple wavelength measurements at seven incident angles. The angles of incidence for evaluation were 50° to 80° in 5° increments with an acquisition time of at least five seconds per angle. Our instrument uses white light (193 to 1000 nm) that is initially linearly polarized. The polarization direction of this linearly polarized light is at 45° from both the s- and p-planes as it strikes the surface. The p-plane contains the surface normal and the direction of ray propagation. The s-plane is perpendicular to the p. As the light reflects, the polarized light amplitudes change according to the formula $\tan\Psi e^{i\Delta} = \frac{r_p}{r_s}$, where the ratio of the Fresnel coefficients $\frac{r_p}{r_s}$ in the p and s directions is related to Ψ (amplitude), and the difference in phase between the two amplitudes is Δ (Figure 2.2)

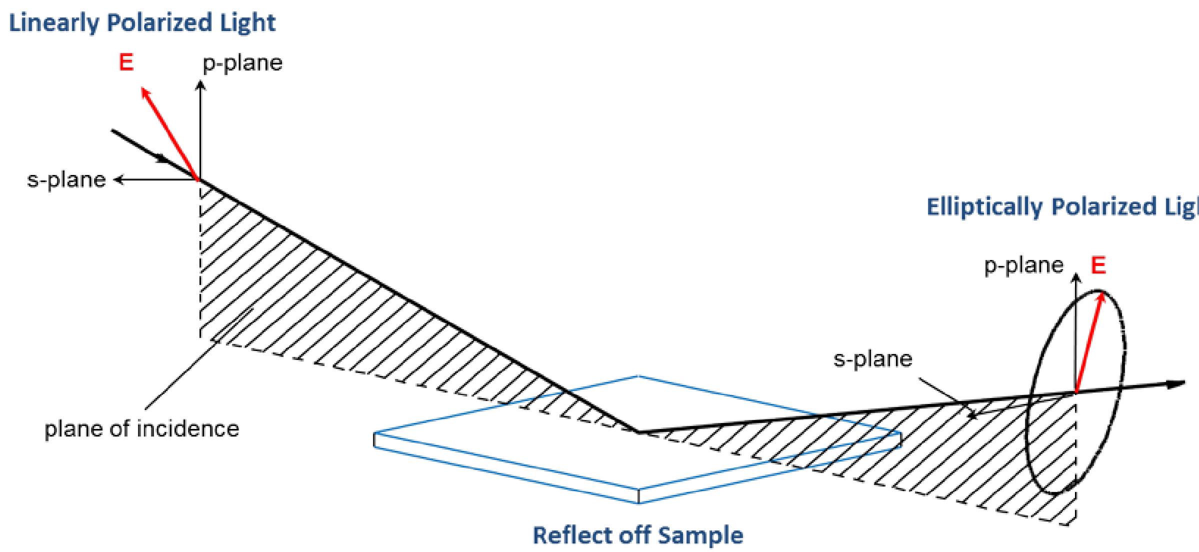

Figure 2.2 Illustration of the polarization change measured in spectroscopic ellipsometry. Incident light that is linearly polarized reflects from the sample surface. Reflection causes a relative amplitude and phase shift that produces elliptically polarized light, which is used to determine film thickness and optical constants. From https://www.jawoollam.com/resources/ellipsometry-tutorial/what-is-ellipsometry

2.4 Ellipsometry modeling (CompleteEASE)

After the ellipsometry data was collected, the measurements were processed using J.A. Woollam's CompleteEase^{TM} software to obtain the film thicknesses and, in some cases, the optical constants of individual layers. Our overall objective in these methods was to extract the approximate layer thicknesses of the top layers of the surface, the MgF_2 layer, as well as that of the alumina layer. To achieve this, a multiparameter model was used to fit layer thicknesses of the thin-film stack corresponding to the experimental Ψ and Δ values, using the CompleteEASE-generated mean squared error (MSE) to evaluate fit quality. This dimensionless MSE value is calculated by minimizing the difference between the experimental measurements and the generated theoretical model, expressed as:

$$MSE = \sqrt{\frac{1}{3n-m}\sum_{i=1}^{n}[(N_{E_i}-N_{G_i})^2+(C_{E_i}-C_{G_i})^2+(S_{E_i}-S_{G_i})^2]} \times 1000 \tag{2.1}$$

where n is the number of wavelengths, m is the number of fit parameters, E and G denote the experimental and generated data, respectively. The remaining terms are defined as $N = \cos(2\Psi)$, $C = \sin(2\Psi)\cos(\Delta)$, and $S = \sin(2\Psi)\sin(\Delta)$ [9]. Ultimately, a lower MSE value indicates a higher quality fit and closer agreement between the theoretical model and the measured experimental data.

When fitting SE data from a dielectric multilayer that contains ultra-thin films with similar refractive indices and dispersion, the computed film thicknesses and roughness are strongly (negatively) correlated. This means that an increase in the fitted film thickness can be offset by a decrease in fitted roughness, and vice versa, while still producing a good match to the measured data. Because these parameters trade off against each other in the model, independently determining the true values becomes more challenging.

To minimize this uncertainty in our study, the values of correlated parameters were constrained by other physical observations and prior knowledge. For example, surface roughness was measured by AFM. The measurements were used to identify surface features and analyze trends in the root-mean-square (RMS) nanoroughness. RMS roughness represents how much the surface height deviates on average from the mean surface level. The AFM measurements were used to define the allowable range of roughness values in the model and to improve the reliability of the fitted film thickness. This is important because errors in these correlated parameters could lead to incorrect predictions of optical performance and prevent an accurate understanding of the true thickness of each thin film.

The indices of AlF_3 and MgF_2 are very similar (for example, 1.398 and 1.386 at 3.3 eV), making it difficult to determine their individual thicknesses. Therefore, we often lumped the AlF_3 and the Al oxide into the MgF_2 as one MgF_2 layer with an ‘apparent’ thickness. When performing VASE analysis, we started by modeling the MgF_2 thin-film layers above the Al as a single dielectric layer.

Therefore, in the first analyses for each sample, only three thicknesses were fit: the apparent MgF_2 layer, the Al layer, and the CVD Si_3N_4 layer.

The optical constants were fitted, but were constrained to be the same for all samples [10]. Only the Al, the MgF_2, and the Si_3N_4 film thicknesses are allowed to differ between samples. It was observed that there was a decrease in the Al thickness in some of the Al+XeMgF_2 samples as peel-off cycles increased. This decrease can be attributed to oxidation of the Al film, producing an aluminum oxide. By measuring the samples multiple times over extended periods of time, we get a better understanding of how a given Al+XeMgF_2 film fares after being cleaned by, and being stored in, each of the four FCP formulations evaluated.

2.5 Atomic force microscopy (AFM)

To constrain the roughness, we performed AFM to provide an initial roughness survey of the surface topology. We acquired three 5 μm $\times$ 5 μm scans and one 10 μm $\times$ 10 μm scan. Sample scans were from random locations with no features visible on the surface from the AFM's optical microscope. The AFM measurements were analyzed in software called Gwyddion [11], from which we acquired an associated RMS value. Large features such as blisters or dust were excluded from the RMS roughness because they would not provide an accurate representation of the true surface roughness. As explained in the previous section, this data was used to constrain the surface roughness in the model.

Chapter 3

Results

In this chapter, we will discuss the AFM results as well as three figures that show how different layers of the thin-film stack changed according to our model. The first figure shows the mean square error versus time. This tells us how well each layer from the thin-film stack (Figure 2.1) fits with the model for each formulation. The next figure will show how each formulation affects the apparent MgF_2 layer. The final figure shows how well each formulation protects the aluminum from oxidation.

3.1 AFM Results

We had a limited number of AFM scans (11) to obtain an initial roughness value for each sample and to understand the morphology after a few applications. Via AFM, the average RMS roughness of all samples at the start of the experiment was 1.17 nm, with a standard deviation of 0.30 nm. After 25 days, the RMS roughness for S1 was 1.26 nm. On day 26, Control 2 had an RMS of 0.96 nm. On day 36, S2 showed an RMS roughness of 1.13 nm. After 46 days, Controls 1 and 2 had an RMS roughness of 0.99 and 1.09 nm, respectively. There are insufficient data to calculate trends for times up to 46 days. However, none of the five RMS values measured later differs from the original average by up to one standard deviation. Four values are smaller, and only one is larger than the initial average. The average of these five measurements is 1.09. Therefore, for the first month and a half, the roughness does not change for controls and the treated samples as measured by AFM.

The SE model used is shown in Figure 2.1, except that the two fluoride layers are combined as one 'apparent MgF_2' layer. To understand our VASE results, we consider the values of three parameters with time: MSE (Fig. 3.1), MgF_2 thickness (Fig. 3.2), and Al_2O_3 thickness (Fig. 3.3). Overall, the application and peel-off of the FCP proceeded smoothly except for formulation S4. For the first couple of applications, the S4 formulation could be easily removed. However, the time came when a visible portion of the Al+XeMgF_2 layer peeled off with the FCP. This is likely due to excessive polymer-to-layer adhesion and/or the inadequate cleaning of the substrate before Al deposition.

3.2 Fit Quality and Modeled Thin-Film Changes

In Figure 3.1, the MSE values remain low for all formulations for the first two peel-off cycles. After that, MSE for S1 began to increase, though the MSE remained below 3 until about day 45. S4 also increased, but the rise was not quite so dramatic, and the MSE varied from cycle to cycle. The other two samples, which are cleaned with formulations S2 and S3, remain low, as do the two controls. In fact, by day 400, the MSE of the two FCP cleaned samples is lower than that of the controls. This provides evidence that these two formulations may be compatible with cleaning the MgF_2 surface many times and that the Al+XeMgF_2 sample can be stored in these formulations.

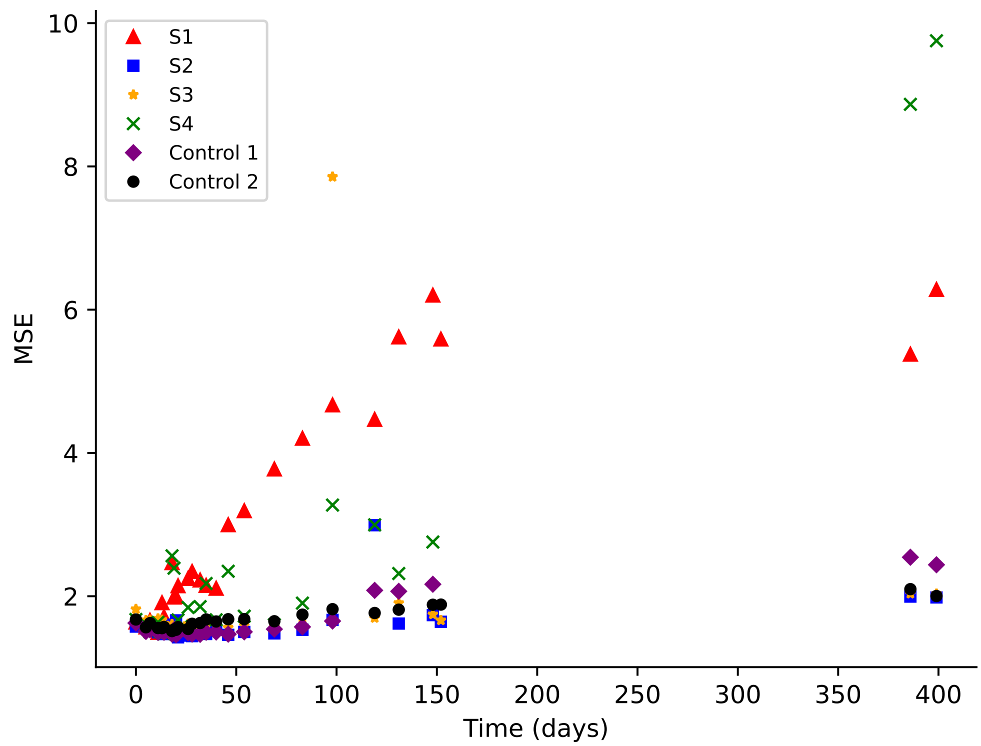

Figure 3.1 Mean squared errors (MSE) from the ellipsometric fit versus peel-off cycles for six Al+XeMgF2 samples. Four FCP formulations (S1-S4) and two controls with no FCP applied (Control 1 and Control 2) are shown. Note that for formulation S1, the MSE increases dramatically around 40 days after the initial application. This indicated that the changes in the Al+XeMgF2 layers are large enough that VASE measurements become unreliable. The single unusually high data point for S3 is likely due to a data collection error rather than a sample effect.

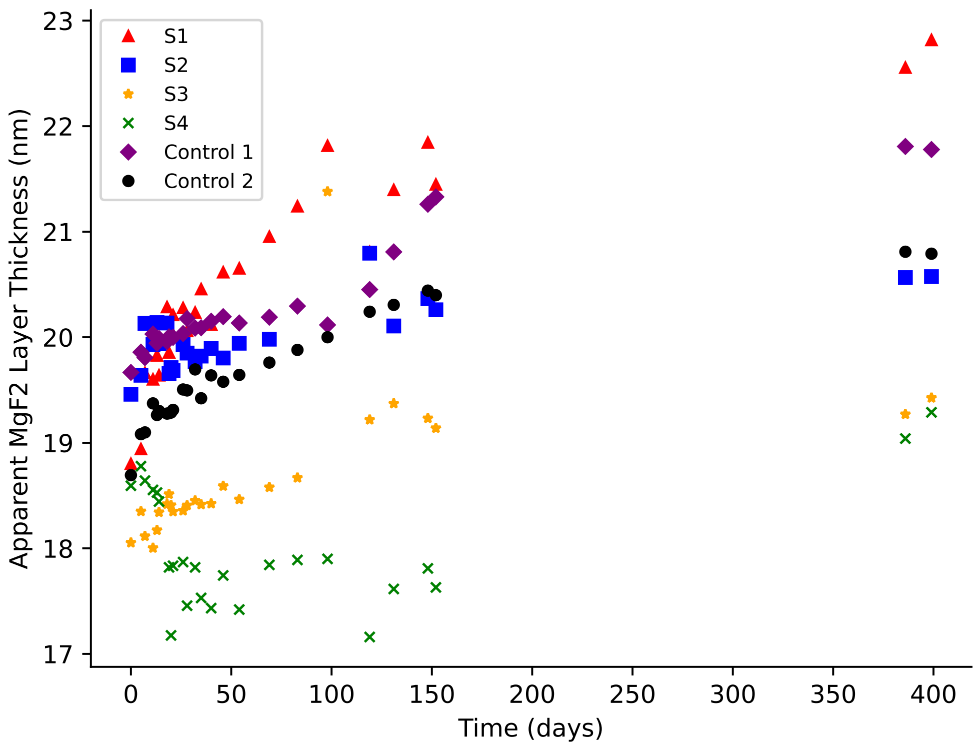

Figure 3.2 Apparent MgF_2 layer thickness for six $XeMgF_2$ thin-film stacks as computed from the VASE model. Each data point was taken after the application and removal of one of the four formulations of FCP for S1-S4. The two controls (Control 1 and Control 2) had no FCP applied, but were removed from desiccator storage and measured at the same time as the others. Each data point corresponds to three measurements across the samples with measurement angles 50° to 80° in 5-degree increments over the spectral range of 193 to 1000 nm. Note that values for S1 are from data that is poorly modeled by the CompleteEASE model used. Also note the dramatic changes in S4 data are likely due to the thin film being damaged during one of the early peel-off cycles. Again, the single unusually high data point for S3 is likely due to a data collection error rather than a sample effect.

Recall that the 'apparent' MgF_2 layer includes the MgF_2, the AlF_3, and the alumina. The initial values for the fluoride thickness are different for each of the six samples. This reflects the fact that they came from different portions of the wafer. The thickness of the layer is highest for portions of the wafer that were closest to the deposition sources. Note that the thicknesses for S2 (squares) and S3 (stars) and the two controls (diamond and circle) are relatively constant with time or trend upward only modestly. The increase in apparent fluoride thickness in MgF_2 layers with time in air was attributed to the deposition of adventitious carbon from air. However, it could also be due to moisture resculpting the surface of the fluoride in the controls. Both processes appear to be blocked in S2. That is, S2 blocks water adsorption on the surface and blocks or removes adventitious carbon.

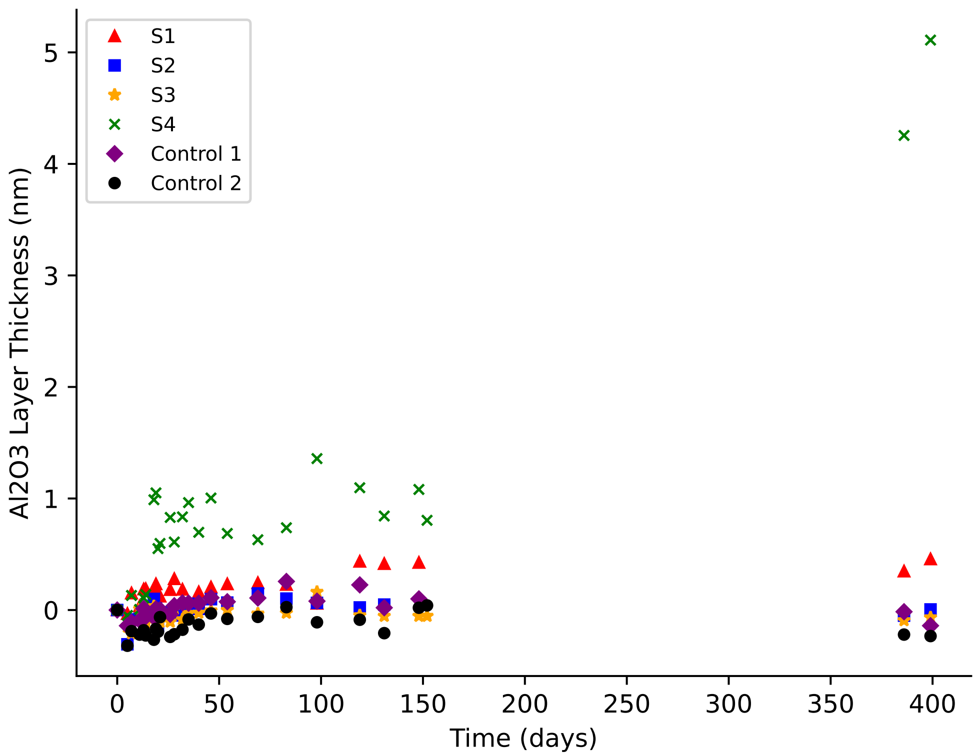

Figure 3.3 Al_2O_3 thickness for six $XeMgF_2$ thin-film stacks as calculated from the VASE model. Each data point was taken after the application and removal of one of the four formulations of FCP for S1-S4. The two controls (Control 1 and Control 2) had no FCP applied, but were removed from desiccator storage and measured at the same time as the others. Each data point corresponds to three measurements across the samples with measurement angles 50° to 80° in 5-degree increments over the spectral range of 193 to 1000 nm. The majority of the samples have little to no Al_2O_3 growth. Note that S4 had large Al_2O_3 growth, likely due to the coating being partially removed along with the first contact during an early peel-off.

The growth of alumina is calculated from the disappearance of aluminum. No alumina growth over time is seen for S2 (squares), S3 (stars), or the two controls (diamonds and circles). Also, note that the alumina thickness jumps up after the 6th peel-off for S4. This is the sample that showed film delamination at the fourth peel-off. You can also see that, due to delamination, the alumina thickness increased dramatically after about 400 days in storage.

Overall, we can see that S2 shows the least amount of change in the apparent MgF_2, which slightly differs from the pattern of the controls. We believe that means that it is protecting the sample. S3 had the least amount of alumina growth, which also points to protection. These two formulations show the best overall results for what we were searching for in this experiment.

Chapter 4

Discussion

We used VASE ellipsometry data to identify which FCP formulations (S1-S4) were capable of successfully cleaning thin Al+XeMgF_2 coatings multiple times. We found that all FCP formulations can be used to clean Al+XeMgF_2 coatings at least once. Formulations S2 and S3 showed promise as acting as a protective coating for Al+XeMgF_2 mirrors for at least thirteen months of storage in dry environments.

Our findings differ from those in similar experiments on Al+XeLiF. For example, Vawdrey's experiment using Al+XeLiF [7] found that all formulations could be used to clean the coatings at least once, but none of the formulations were suitable for storage with multiple peel-offs. In contrast, our results indicate that Al+XeMgF_2 appears to be compatible with both storage and repeated cleaning using FCP formulations S2 and S3. These coatings are promising candidates for future space telescope mirrors because protection against contamination and degradation increases FUV reflectivity.

Formulation S1 showed some changes in the MgF_2 layer that could indicate roughening or surface damage, which is potentially detrimental to the surface. Degradation with formulation S4 may also indicate that polymer-to-surface adhesion is too high for the Al+XeMgF_2 film surfaces.

Giving attention to ensuring good cleaning to promote adequate adhesion before deposition may help address this issue.

It should also be noted that the top layer of our thin-film stack appeared to change since the ellipsometry model lumped several thicknesses into the top layer. This could include swelling in the MgF_2 layer due to recrystallization, retention of water in between MgF_2 and AlF_3 crystals, surface damage, or other changes in roughness not captured by AFM. Refinement of our ellipsometry model would need to be done to understand exactly what is occurring.

The Al layer thickness in the coatings studied is only 30% of the flight mirror thickness and 70% of the target fluoride layer. Studies on fully thick mirrors still need to be completed. Future FUV reflectance measurements should also be performed.

Formulations S2 and S3 would be useful starting points for Al+XeMgF_2 storage and cleaning. An optimal polymer for Al+XeMgF_2 mirrors would need to ensure that polymer-to-surface adhesion is in the range to remove contaminants without causing Al+XeMgF_2 surface damage. Future work is needed to test the current or new formulations for storing MgF_2 at higher relative humidity, for example, at 40% relative humidity, which is characteristic of cleanrooms and environments where electronics are used.

Bibliography

[1] David D. Allred et al. "Adding EUV reflectance to aluminum-coated mirrors for space-based observation". In: *UV/Optical/IR Space Telescopes and Instruments: Innovative Technologies and Concepts VIII*. Vol. 10398. 34. SPIE, Sept. 5, 2017. ISBN: 9781510612532. DOI: 10.1117/12.2274694.

[2] Jason Tumlinson et al. "Light and Metals from Population III Stars". In: *ESO Astrophysics Symposia*. Springer, Berlin, Heidelberg, Sept. 22, 2003, pp. 185–186. DOI: 10.1007/10719504_32.

[3] Manuel Quijada et al. "Enhanced far ultra-violet optical properties of physical vapor deposited aluminum mirrors through fluorination". In: *Space Telescopes and Instrumentation 2024: Ultraviolet to Gamma Ray*. SPIE, Aug. 21, 2024, p. 152. DOI: 10.1117/12.3021592.

[4] Patricia Hansen, Jacqueline Townsend, and Randy Hedgeland. "Lessons Learned from the Hubble Space Telescope (HST) Contamination Control Program". In: *Journal of the IEST* 50.1 (Apr. 11, 2007), pp. 44–60. DOI: 10.17764/jiet.50.1.c7835r3280617256.

[5] Brian I. Johnson et al. "Oxidation of aluminum thin films protected by ultrathin MgF2 layers measured using spectroscopic ellipsometry and X-ray photoelectron spectroscopy". In: *OSA Continuum* 4.3 (Feb. 25, 2021), pp. 879–895. DOI: 10.1364/osac.417302.

[6] Joshua Vawdrey, James Hamilton, and David Allred. "Variable-angle, spectroscopic ellipsometry study on the repeated application of first contact polymer on silicon-based surfaces".

In: *Current Developments in Lens Design and Optical Engineering XXIV*. Vol. XXIV. SPIE, Oct. 2, 2023, p. 24. DOI: 10.1117/12.2692390.

[7] Joshua Vawdrey et al. "Effect of the repeated application of First Contact™ polymer on xenon-difluoride passivated lithium fluoride on aluminum surfaces for space telescopes". In: *J. Vac. Sci. Technol. A* 43.43408 (2025). DOI: 10.1116/6.0004601.

[8] John Woollam et al. "Overview of variable-angle spectroscopic ellipsometry (VASE): I. Basic theory and typical applications". In: *SPIE Proceedings*. SPIE, July 19, 1999. DOI: 10.1117/12.351660.

[9] *CompleteEASE Data Analysis Manual*. Accessed: April, 2026. J.A. Woollam Co., Inc. URL: https://physlab.lums.edu.pk/images/f/f4/Ellipsometry_manual.pdf.

[10] Dhruv Shah et al. "Optical function of atomic layer deposited alumina (0.5–41.0 nm) from 191 to 1688 nm by spectroscopic ellipsometry with brief literature review". In: *Surface Science Spectra* 26.2 (Dec. 17, 2019). DOI: 10.1116/1.5114827.

[11] David Nečas and Petr Klapetek. "Gwyddion: an open-source software for SPM data analysis". In: *Open Physics* 10.1 (Oct. 13, 2011), pp. 181–188. DOI: 10.2478/s11534-011-0096-2.

Index